Journal of Polymers and the Environment
https://doi.org/10.1007/s10924-020-02002-4

ORIGINAL PAPER

Cellulose Schiff Base as a Bio-based Polymer Ligand: Extraction, Modification and Metal Adsorption Study

Omid Jawhid[1] · Neda Seyedi[2] · Gholam Hossein Zohuri[1] · Navid Ramezanian[1]

Accepted: 28 November 2020

Abstract

Cellulose was initially extracted from Safflower (*Carthamus tinctorius* L.) stem wastes and used for the preparation of a fully bio-based adsorbent polymer Schiff base (Sch) using oxidation reaction of the extracted compound. A safe cross-linked cellulose dialdehyde (CC-DA) was subsequently synthesized through epichlorohydrin (ECH) and sodium metaperiodate followed by Sch formation with *p*-phenylenediamine (*p*-PDA). All of the reactions carried out including cross-linking, oxidation, and Sch formation of the extracted cellulose were confirmed via Fourier-transform infrared spectroscopy (FTIR) study. The microstructure of the modified products was also investigated using scanning electron microscopy (SEM). The prepared modified cellulose was further characterized by X-ray powder diffraction (XRD), mapping, energy-dispersive X-ray spectroscopy (EDX), CHNS, and thermogravimetric analysis (TGA). Furthermore, it was used in the removal of Pb(II) from wastewater. The effect of some factors such as pH, contact time, and adsorbent dosage was additionally examined in batch mode experiments. Maximum removal efficiency of Pb(II) reached 98.5% at pH 6 and the contact time of 15 min. The kinetic analyses revealed that the adsorptions of Pb(II) on the cellulose Sch adsorbent followed with a pseudo-second order model ($R^2 > 0.99$). Moreover, the adsorption isotherms were well fitted with the Langmuir isotherm, suggesting that homogeneous monolayer surface adsorption that had occurred. The spontaneous and endothermic nature of the adsorption process was further settled by thermodynamic parameters.

Keywords Extracted cellulose · Cellulose oxidation · Cellulose Schiff base · Metal biosorbent

Introduction

As the population grows, global demands of fresh-water for food preparation and agricultural operations are steeply rising [1]. On the other hand, water pollution is one of the most important threats to human health [2]. Accordingly, arsenic, cadmium, chromium, copper, nickel, lead and mercury, even in minor quantities, are the most inorganic water pollutant [3]. Among these ions, Pb toxicity also called lead poisoning is an important environmental disease, which can affect human existence and even animals if consumed above certain threshold concentrations [4]. Various industries including paint, batteries, metal plating, insecticides, cosmetics, alloys, and mining are also among the most significant sources releasing heavy metals into water [5]. As it is not possible to prevent the improvement of these industries and their resulting wastes, it seems necessary to make use of approaches towards removing the mentioned heavy metals as much as possible. Numerous research studies have been conducted in this area. In this regard, the safety of applied methods and materials as well as their high efficiency, due to the vastness of industries, has been required [6–8]. In general, the adsorption technique is one of the widely used processes for removal of heavy metals, since it is highly effective and reasonably inexpensive [9]. Various materials such as activated carbon and carbon based materials [10–16] natural zeolite [17–20], bentonite clay [21, 22], red mud

Supplementary Information The online version contains supplementary material available at https://doi.org/10.1007/s10924-020-02002-4.

✉ Neda Seyedi
Nedaseyedi@ujiroft.ac.ir

✉ Gholam Hossein Zohuri
zohuri@um.ac.ir

[1] Department of Chemistry, Faculty of Science, Ferdowsi University of Mashhad, Mashhad, Iran

[2] Department of Chemistry, Faculty of Science, University of Jiroft, Jiroft, Iran

Published online: 02 January 2021

[23], polymers and biopolymers [24–27], fly ash [28], biomasses [29] and metal oxid nanoparticles [30–39] have been accordingly evaluated for removal of the heavy metals and other pollutants. Due to their high surface area and environmentally friendly properties, biopolymers can be similarly found the best choice for this process [40].

Cellulose is known as the most attractive one, among other bio-based polymers, found naturally. It is renewable, environmentally friendly, efficient and cost-effective, sustainable, and biodegradable [41]. This organic compound can be also easily derived from plant sources and the most abundant biological macromolecules with numerous hydroxyl groups that are receptive to chemical modifications [42–44]. Therefore, it can be a good substrate for adsorption reactions. However, its poor reactivity and slow removal rate are the main limitations facing its adsorption applications [45, 46]. Chemical modification of the molecular structure of cellulose to improve its physical and adsorption efficiency has been accordingly drawing researchers' attention in recent years [47].

Modification of cellulose chains via division of the C_2–C_3 bond between vicinal hydroxyl groups has resulted in the formation of two aldehyde groups per glucose unit [48–50]. Periodate oxidation also relies on a one-pot synthesis in aqueous solutions which can be easily stopped using some ethylene glycol [51]. The synthesized polymer containing aldehyde groups can be further converted into other functionalities such as carboxylic acid, sulfonic acid, amino acid, hydroxyl, or can be reacted with a primary amine to form a Schiff base [47]. The chelating groups on the cellulose chains can also act as active sites for removal of the heavy metal ions from aqueous solutions [52]. This study reflected on the extraction cellulose from dried stem powder of Safflower (*Carthamus tinctorius* L.).

The novelty of this study is that it highlights the possibility of integrated use of extracted biopolymer from biomass in the heavy metal adsorption from wastewater. A simple, efficient, and new method have been developed for the extraction of cellulose from dried stem powder Safflower (*Carthamus tinctorius* L.). To prepare an efficient new high surface biosorbent for metal ions, the extracted cellulose was cross-linked, periodate oxidized, and then functionalized with *para*-phenylenediamine (*p*-PDA) to develop chelating sites between the polymeric chains. The produced cross-linked cellulose (CC)-Sch was then evaluated as a biosorbent for lead(II) nitrate ions from contaminated water. The effects of pH, contact time, and adsorbent dosage were subsequently investigated in batch mode experiments. This novel biosorbent exhibits high efficiency for lead adsorption and the values of TOF and TON are found to be within the range of millions which are ideal cases for the industrial-scale applications.

Experimental

Materials

Glacial acetic acid and potassium hydroxide were purchased from Panreac Quimica S.A.U (Spain) and Merck Co. (Germany); respectively. Epichlorohydrin (ECH) came from Riedel De Haen AG Seelze Hannover (Germany). Sodium metaperiodate was bought from BDH Chemicals Ltd. Poole (UK). Sodium chlorite (80%) and *p*-PDA were obtained from the technical grade of Sigma-Aldrich Co. (Germany). Moreover, distilled water was used in this study.

Cross-Linking of Extracted Cellulose

Safflower stem wastes were washed, sun-dried, powdered and then cellulose extraction process was implemented following instructions in authors' previous work [53]. The extracted cellulose (6 g) was dispersed into water (100 mL) under sonication and continuously stirred at room temperature (30 min). Subsequently, an aqueous solution of sodium hydroxide (50 mL, 22%) was added to the reaction container. After mixing (for 50 °C, 2.5 h), ECH (40 g) and ammonium hydroxide (45 g, 25% solution) were added and the reaction mixture refluxed (for 4.5 h, at 55 °C). The product was washed (three times) with ethanol and distilled water and dried for 15 h (at 60 °C) [54].

Preparation of CC-Sch

CC (4 g) was immersed in distilled water (100 mL) and oxidized with $NaIO_4$ (6 g) in a dark atmosphere. After 3-h stirring (at 55 °C), oxidation was stopped by adding an excess of ethylene glycol followed by filtering and washing of C-DAC with ethanol and water. The prepared C-DAC (6 g) reacted with *p*-PDA (6 g) at 70 °C for overnight (Fig. 1). The product was filtrated and washed with toluene and dried (for 12 h, at 50 °C).

Adsorption Experiments

The metal ion adsorption study of CC-Sch base adsorbent was evaluated using an aqueous solution of Pb(II). All the experiments were performed in a glass container (100 mL) under shaking (at 200 rpm). The effect of different parameters such as adsorption dosage (0.2–4 mg/mL), pH value (2–10) adjusted by addition of hydrogen chloride (0.1 M) or NaOH (0.1 M), metal ion concentration (30–100 ppm), and contact time (5–25 min) were then investigated. After each adsorption experiment, the adsorbent was separated from the reaction mixture by

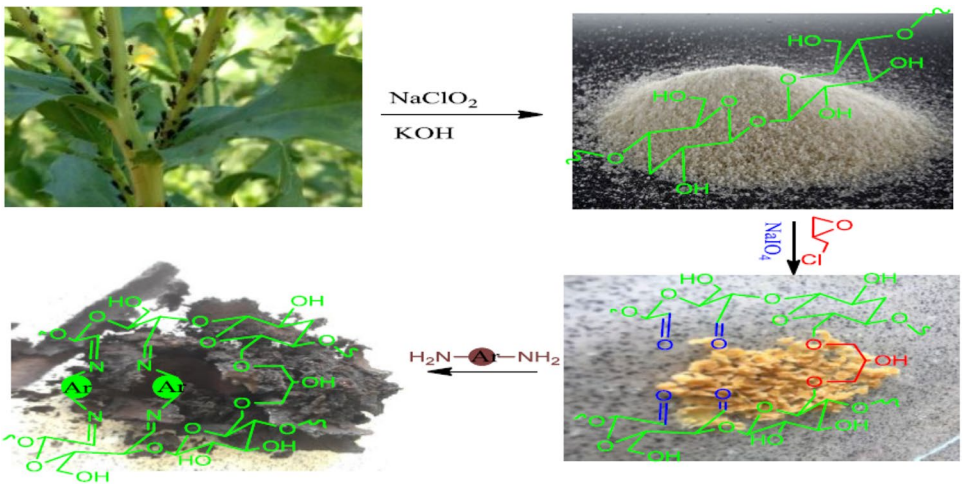

Fig. 1 Scheme of green polymer CC-Sch preparation process

centrifuging and the residual solution analyzed for metal ion concentration through an atomic adsorption spectrophotometer (AAS) (Perkin Elmer Analyst 400). Removal efficiency (R) and equilibrium adsorption efficiency (Qe) of heavy metal ions (mg heavy metal ion/g adsorbent) were ultimately determined according to Eqs. 1 and 2 [52]:

$$R(\%) = \frac{(C_0 - C_e)}{C_0} \times 100 \quad (1)$$

$$q = \frac{(C_0 - C_e)V}{m} \quad (2)$$

wherein C_e and C_0 (mol. L^{-1}) represent equilibrium and initial concentrations; respectively. V also shows solution volume and m indicates weight of adsorbent (g).

Results and Discussion

Characterization of Cellulose Adsorbent

The FT-IR spectra of CC, CCDA and CCS-ch are shown in Fig. 2. The index bands of the modified cellulose extracted spectra at 3419, 1727, 1163, and 1060 cm^{-1} were attributed to hydrogen bonded of –OH groups, C=O stretching, C–O vibration, and C–O–C stretching; respectively. Upon *p*-PDA treatment, the spectrum of CC-Sch presented a new peak at approximately 1513 cm^{-1} and 1260 cm^{-1}, which could be ascribed to C=N and C–N bending vibration of Sch formed between aldehyde groups of the oxidized cellulose and the amino groups of the *p*-PDA [54].

Microstructure and surface morphology of the synthesized product surface was further investigated from SEM images (Fig. 3). The image of the extracted cellulose exhibits arranged cellulose chains due to the strong intramolecular hydrogen bonding (Fig. 3a). Surface morphology also

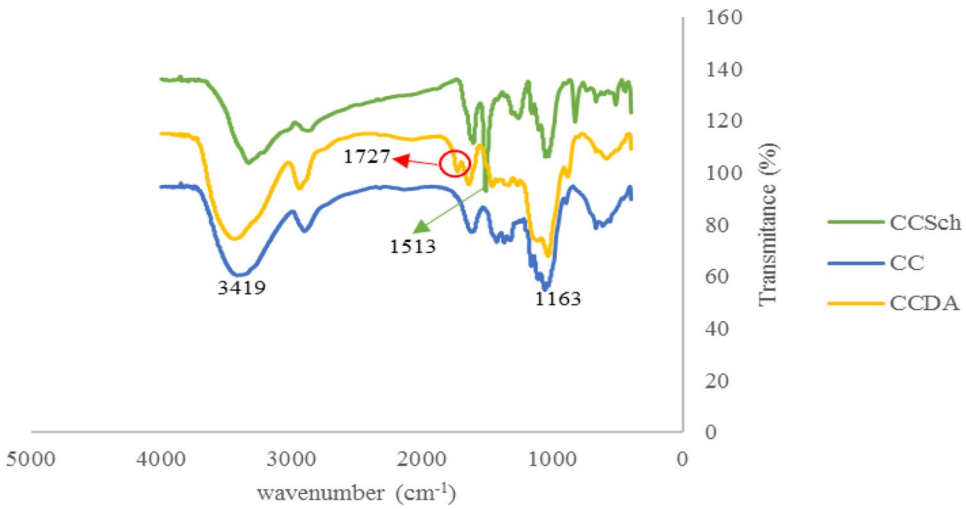

Fig. 2 FTIR spectrum of modified cellulose

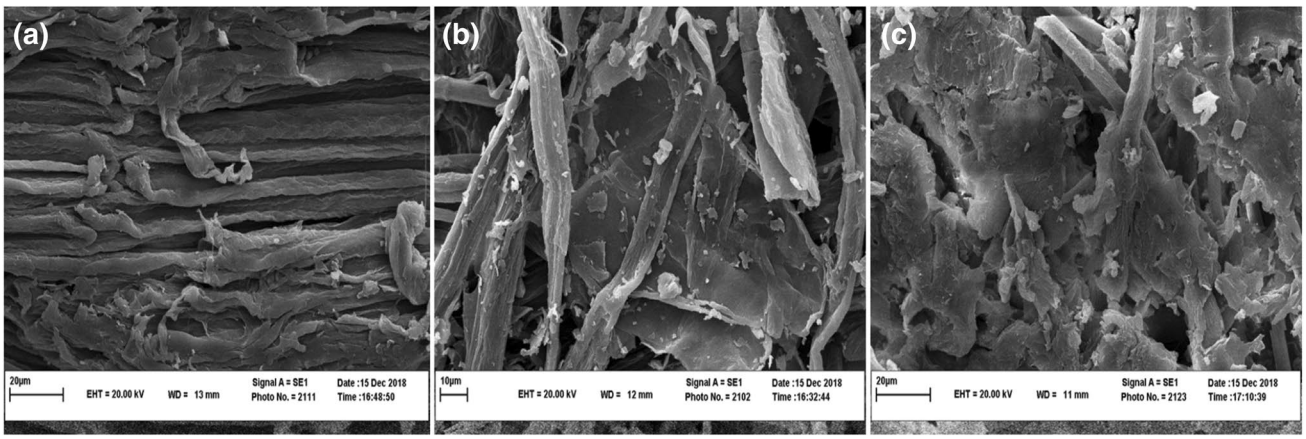

Fig. 3 SEM images of **a** cellulose, **b** CC, and **c** CC-Sch

resulted from the proximity of different cellulose chains after cross-linking (Fig. 3b). However, the surface of CC-Sch seemed rougher and wider compared with CC-DA following *p*-PDA grafting (Fig. 3c) [55]. The presence of C, N and O in the CC-Sch has been proved by EDX analysis and mapping (S1, S2).

And also, The CHNS analysis of the CC-Sch is presented in Fig. S3. Wherein the element composition of carbon is (56.69%) and hydrogen (5.33%) and an additional peak due to N (8.79%) which also confirms functionalization of CCDA with *p*-PDA.

The thermal behavior of the CC-Sch was analyzed (Fig. S4). Thermal analysis of the CC-Sch has proved to be useful in determining the structure of cellulose and thermal stability as well as the decomposition mode under controlled heating rate [56]. As observed, the peak with 3.6% mass loss at 63 °C about the loss of moisture. Two main degradation steps with 16.2% weight loss in the CC-Sch are observed and produced at 200 °C and 312 °C because of dehydration and depolymerization-tar-forming processes in cellulose. The CC-Sch showed relatively higher stability that could be due to the crosslinking and the inclusion of phenyl groups in the structure. And also CC-Sch did not show any degradation below 200 °C, and therefore, can act as an effective resistant biogradable adsorbent in heavy metal adsorption reaction.

The X-ray diffraction (XRD) pattern of the CC-Sch indicated low intensity and a broad diffraction peak (Fig. S5), which clearly confirmed an amorphous structure [57, 58]. However, the XRD pattern of crystalline cellulose used in previous reports was showed sharp peaks at $2\theta = 15°$, 20.3°, and 22.2°, corresponding to the $(1\bar{1}0)$, (110), and (200) planes, respectively, something that is absent in the XRD spectra of our synthesized cellulose [57].

Cellulose Adsorbent for Removal of Heavy Metals

Effect of Adsorbent Dosage

Figure 4 shows the effect of adsorbent dosage on Pb(II) removal by CC-Sch adsorbent. In this study, adsorbent

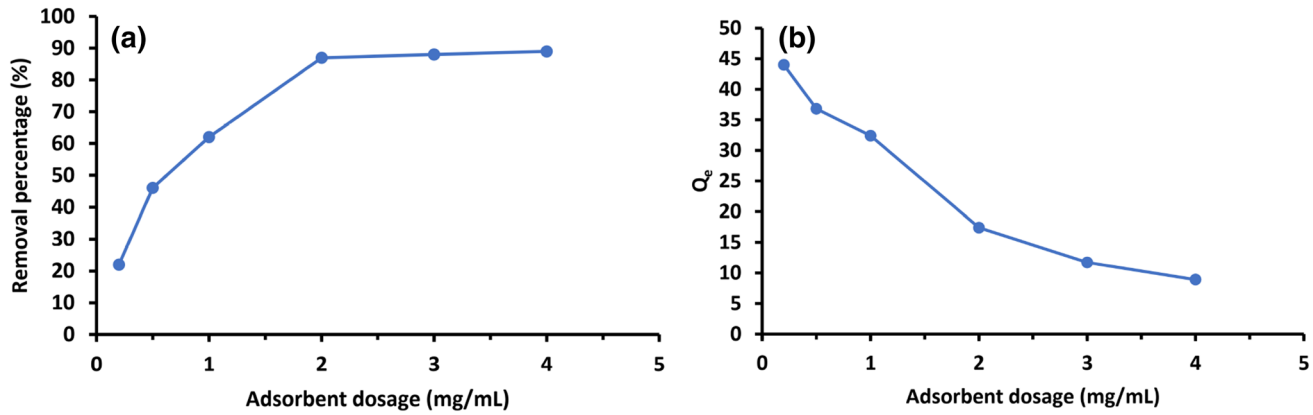

Fig. 4 Effect of adsorbent dosage on Pb(II) adsorption

dosages of 0.2–4 mg/mL were added to Pb(II) solution (50 mL, 20 mg/L) and shaken (for 10 min, at room temperature). As observed in Fig. 4a, the amount of R increased with increasing of CC-Sch base adsorbent dosage (from 0.2 to 2 mg/mL), due to the growth in the number of available adsorption sites for metal ion binding and it reached to 87% by using of adsorbent dosage higher than 2 mg/mL. The behavior could be as a result of the equilibrium of the metal ion concentration on the surface of the adsorbent and in the solution [59]. On the other hand, the adsorption efficiency decreased dramatically as the adsorbent dosage was augmented (Fig. 4b). The reason was mainly connected to unsaturated adsorption sites through adsorption reaction and particle interactions, such as aggregation, resulting from high adsorbent concentration [60]. In addition, such aggregations would lead to a decrease in the total surface area of the adsorbent [61].

Effect of pH

pH is typically a parameter affecting the adsorption of heavy metal ions in its process. The experiments were accordingly conducted with adsorbent dosage (2 mg/mL) in aqueous solution (50 mL) containing Pb(II) (40 ppm) which was shaken at room temperature (for 10 min) over the pH range of 2–10. Based on Fig. 5, the R (removal efficiency) of Pb (II) significantly increased as the pH of the solution was raised. Maximum R also reached 98.5% at pH 6.5. Under acidic conditions, the predominant metal species M^{2+} and $M(OH)^{+}$ were positively charged and the imine and other functional groups of adsorbents were protonated and the charge on the surface of the adsorbent became positive. Therefore, there was a significant electrostatic repulsion between the cationic Pb(II) ions and positively charged functional groups on the surface of the adsorbent, inhibiting the adsorption of Pb(II). In addition, the competitive uptake of H^{+} cations was considered to be the reason for the lower up taken of the metals in more acidic environments. On the other hand, a subsequent decrease in R at a pH value higher than 6.5 could be due to the formation of Pb hydroxides in the solution. Thus, an optimum pH value of 6.5 was chosen for further batch adsorption studies.

Effect of Contact Time

Adsorption of Pb(II) onto the cellulose-based adsorbent as a function of time was studied under pH of 6.5, initial Pb(II) concentration of 40 ppm, adsorbent dosage of 2.0 mg/mL at room temperature as shown (Fig. 6). The results indicated that the adsorption rate was very initially fast (the amount of Pb adsorption in 5 min was about 69%) could be due to the availability of coordination sites, and reached a limiting value (98.5%) after 15 min of the reaction. Hence, it was chosen for further studies.

Adsorption Kinetics

The kinetics of the adsorption data was analyzed using pseudo-first-order and pseudo-second-order models to investigate physical–chemical aspects of the adsorption process of Pb(II) onto the CC-Sch adsorbent. The linear form of both the pseudo-first-order reaction and the pseudo-second-order model are expressed as reported [62–65].

Kinetic parameters are shown in Table 1. Once the experimental data were plotted for both pseudo-first-order and pseudo-second-order kinetics in Fig. 7, the R^2 of the pseudo-second-order models (0.99) regarding Pb(II) adsorption was greater than that for the first–second-order models (0.95). In addition, the calculated q_e values from the pseudo-second-order model (q_e, cal) were very close to the experimental q_e values, indicating that the adsorption process of metal ions on the CC-Sch base adsorbent had followed the pseudo-second order. This confirmed that the Pb(II) concentration

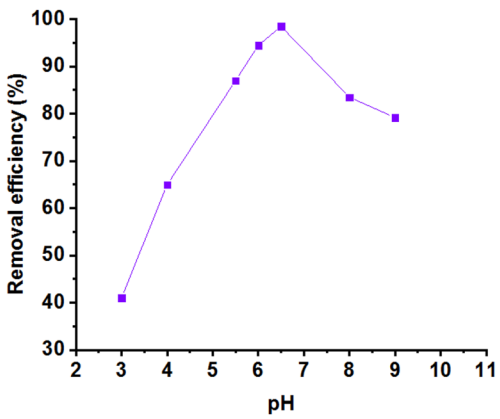

Fig. 5 Effect of pH on R of Pb(II) onto CC-Sch adsorbent: 2 mg/mL; concentration of metal ions: 40 mg L^{-1}; temperature: 298 K

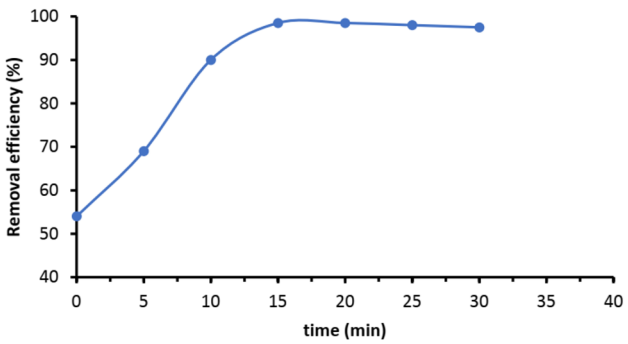

Fig. 6 Effect of time on adsorption of Pb(II); adsorbent: 2 mg/mL; concentration of metal ions: 40 mg L^{-1}; pH: 7.3; temperature: 298 K

had been affected in the rate-determining step in the adsorption process, which might be chemical adsorption [66, 67].

Adsorption Isotherms

Langmuir (Eq. 3) and Freundlich (Eq. 4) isotherm models were applied to describe the adsorption process of Pb(II) on the CC-Sch adsorbent. In this study, the effect of Pb(II) concentration on the adsorption capacity was investigated at different concentrations of 30–100 ppm under the obtained optimized conditions. The Langmuir model assumes that adsorption is monolayer on the homogeneous outer surface of the adsorbent and represents the equilibrium distribution of metal ions between solid and liquid phases [68].

$$\frac{C_e}{q_e} = \frac{C_e}{q_m} + \frac{1}{k_l q_m} \tag{3}$$

where C_e is the equilibrium concentration of metal ion (ppm), q_e refers to the amount of adsorbate adsorbed per unit mass of cellulose-based adsorbent at equilibrium (mg/g), q_{max} shows theoretical maximum monolayer adsorption capacity of the adsorbent (mg/g), and K_L represents the Langmuir isotherm constant related to the adsorption energy (L/mg). As well, q_m and K_L were determined from the plots of C_e/t vs. C_e.

In contrast to the Langmuir model, the Freundlich model assumes that the adsorbent surface energy is heterogeneous with active sites having non-uniform energies (Eq. 4) [69].

$$logq_q = logk_F + \left(\frac{1}{n}\right) logC_e \tag{4}$$

in which K_f is the Freundlich capacity constant and n shows adsorption intensity. q_e and C_e are also the same quantities used in the Langmuir isotherm [70]. This model is typically employed to describe multilayer adsorption on a heterogeneous surface.

The calculated parameters such as R^2, K_L, Q_m, K_F, and n, corresponding to each model are summarized in Table 2. Based on the fitting results, all the R^2 values from the Langmuir model (0.9991) were much greater compared with those for the Freundlich isotherm model. Therefore, adsorption is a homogeneous monolayer process. Besides, the adsorption capacity of the present work is rather than other reported adsorbents that summarized in Table 3. These

Table 1 Calculated parameters for pseudo-first-order and pseudo-second-order models of Pb(II) adsorption on CC-Sch adsorbent (pH 7.35, t = 25, initial concentration of heavy metal ions: 40 ppm and 2 mg/mL. adsorbent)

Metal ion	$q_{e,exp}$ (mg/g)	Pseudo-first-order kinetics			Pseudo-second-order kinetics		
		$q_{e,cal}$ (mg/g)	k_1 (1/min)	R^2	$q_{e,cal}$ (mg/g)	k_2 (g/mg min)	R^2
Pb(II)	19.7	7.73	0.11	0.95	19.84	9.4×10^{-2}	0.99

k_1 (g/mg min): the rate constant of the pseudo-first-order adsorption, k_2 (g/mg min): the adsorption rate constant of pseudo-second-order adsorption q_e and q_t (mg/g) are the amounts of adsorbate adsorbed at equilibrium e and at any time t (min), respectively

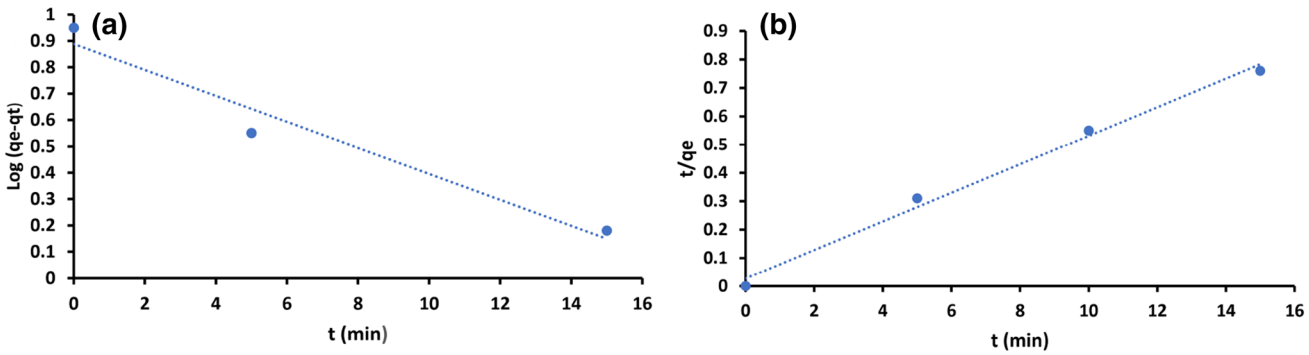

Fig. 7 Pseudo-first-order (**a**) and pseudo-second-order models (**b**) for Pb(II) ion on CC-Sch adsorbent

Table 2 Parameters of the Langmuir and Freundlich models of Pb(II) adsorption on CC-Sch adsorbent

Metal ion	Langmuir isotherm parameters			Freundlich isotherm parameters		
	q_m (mg/g)	K_L (L/mg)	R^2	n	K_F (g/g)	R^2
Pb(II)	33.33	0.583	0.9991	5.56	18.83	0.8412

Table 3 Comparison of adsorption capacities of various adsorbents for removal of heavy metal ions

Adsorbent	q_m (mg g^{-1})	Concentration of adsorbent (g L^{-1})	Contact time (min)	Refs.
Cellulose/GO composite	39.22	2.5	60	[71]
Nanocellulose fiber	9.42	10.35	40	[72]
Chitosan beads	39	5	80	[73]
Cross-linked chitosan–clay beads	7.930	10	80	[74]
Dyed cellulose materials (coir)	26.29	20	4 h	[75]
Cellulose–g-GMA-imidazole	75	3.64	2 h	[76]
MWCNTs/PAAM	29.71	0.4	24	[77]
CC-Sch adsorbent	33.33	2	15	Present study

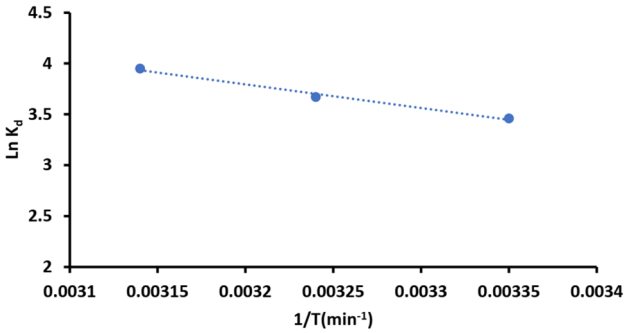

Fig. 8 Linear plot of ln k_d vs. 1/T for adsorption of Pb(II)ion on CC-Sch adsorbent

Table 4 Thermodynamic parameters of Pb(II) ion adsorption on the cellulose Schiff base adsorbent

Metal ions	T (K)	ΔG (kJ/mol)	ΔS^o (J (K^{-1}/mol))	ΔH^o (kJ/mol)	R^2
Pb(II)	298	− 8.65	93.43	19.39	0.99
	308	− 9.55			
	318	− 10.61			

results demonstrated that the CC-Sch adsorbent could be a promising adsorbent for removing Pb(II) from wastewater.

Adsorption Thermodynamics

To assess adsorption thermodynamics, the impact of temperature on R was evaluated at various temperatures (298 K, 303 K, and 318 K) under the optimized obtained conditions. The thermodynamic parameters (Gibbs energy (ΔG^0), enthalpy (ΔH^0), and entropy (ΔS^0)) were further considered [78].

The thermodynamic parameters for the adsorption process are determined from the slope and the intercept of the plot of *ln* K_d vs. *1/T* (Fig. 8) and the results are reported in Table 4. The endothermic nature of the adsorption process was correspondingly confirmed by the positive value of ΔH^0 [79]. Furthermore, the positive ΔS was observed as temperature increased, indicating a higher degree of metal ion freedom at the solid/solution interface driven by the adsorption process [80].

The negative values of ΔG^0 showed that the adsorption reaction was spontaneous. The growth in the negativity of ΔG^0 with higher temperature confirmed that favorability had boosted with temperature [81].

The adsorption mechanism of Pb(II) ions on the CC-Sch adsorbent was studied. Reportedly, chemical adsorptions are the main factor of metal ions adsorption on the cellulose surface [82, 83]. The kinetics experiments in this research revealed that the adsorption of Pb^{2+} on the surface of CC-Sch sorbent is chemical adsorption by electrostatic attraction between heavy metal ions and CC-Sch sorbent. Electrostatic cationic attractions between metal ions and CC-Sch adsorbent were in "Effect of pH" section. Meanwhile, the isothermal study verified that the adsorption of Pb^{2+} onto CC-Sch is a homogeneous monolayer adsorption process. Formation of complexes between metal ions and functional groups is an important factor in metal ion adsorption on the adsorbent surface which is confirmed in this study ("Adsorption Isotherms" section).

The FT-IR analysis of modified cellulose for before and after adsorption of Pb^{2+} were compared to further identify the metal ion-functional group complexes (Fig. S6). Significant changes and shifts of characteristic peaks in FT-IR spectra of CCS-ch adsorbent after metal loading confirm that those functional groups-contained these bonds have involved in the complexes with metal ions.

TON and TOF

The turn over frequency (TOF) is a factor for investigation of the CC-Sch efficiency as a promising adsorbent material and estimated based on the derivative of the number of turnovers of the adsorption cycles in accordance to the time per active surface site on the surface of adsorbent. All the operational conditions which influence the adsorption

behavior of CC-Sch are properly declared and accounted for the estimation of the TOF [84]. In most cases a good approximation method for the estimation of TOF at a specified temperature can be obtained by applying the energetic span approximation (Eq. 5) [85, 86].

$$TOF = \frac{K_b T}{h} e^{\frac{\delta E}{RT}} \quad (5)$$

in which K_b, h, and δE represent the Boltzmann constant (1.38 × 10–23 J/K), Planck's constant (6.63 × 10–34 J s).

Note that δE (the energetic span), being the apparent activation Gibbs energy of the cycle, can be decomposed to $\delta E = \Delta H - T\Delta S$ and, similar to the van't Hoff equation. In the energetic span estimation, the entropy term from the van't Hoff's equation is removed and only the apparent activation enthalpy of the adsorption cycle remained which can be directed to the neglecting the influence of the reaction molecularity on the estimation of the energetic span. Additionally, to predict the maximum utilization of the CC-Sch for the Pb^{2+} adsorption under the defined specific operation conditions including the temperature and pressure by the number of the adsorption cycles up to the decomposition or decay CC-Sch for the efficient Pb^{2+} adsorption, the turnover number (TON) has been estimated by using the following equation (Eq. 6).

$$TON = \frac{TOF \times t_{1/2}}{ln\,2} \quad (6)$$

In which, $t_{1/2}$ represent the half time (sec.) of the adsorption cycle. The results of the TOF and TON are shown in (Table 5). From the findings, it can be seen that the values of both TOF, as well as TON, are found to be within the range of millions which are in accordance with the reported literature. These values are ideal cases for the industrial-scale applications [87, 88].

Conclusion

The present study assessed the process of obtaining new functional cellulose-based biosorbents from stem waste biomasses. The extracted cellulose was successfully cross-linked, simply periodate oxidized, and functionalized with chelating agent (i. e. *p*-PDA). The chemical structure and the morphology of the materials were studied using FTIR, SEM. The prepared functional polymer was then evaluated as an adsorbent of the metal ion Pb(II) from wastewater. By adding to the synthesized adsorbent dosage (from 0.2 to 2 mg/mL), the amount of R increased to 87% through adsorbent dosage of 2 mg/mL. As well, an excellent R (98.5%) was obtained at a pH value of 6.5 at room temperature. The thermodynamic data indicated that the adsorption process was exothermic and spontaneous in nature at various temperatures. The obtained results indicated that the chemically functionalized cellulosic products could be utilized as alternative adsorbents for the removal of lead ions in wastewater sewage.

Table 5 TON and TOF of Pb(II) ion adsorption on the cellulose Schiff base adsorbent

Sample	Temperature (K)	TOF (min^{-1})	TON
CC-Sch	298	$8.23 \times 10^{+7}$	$89 \times 10^{+7}$
	308	$8.50 \times 10^{+7}$	$92 \times 10^{+7}$
	318	$8.78 \times 10^{+7}$	$94 \times 10^{+7}$

Author Contributions All authors have participated in (a) conception and design, or analysis and interpretation of the data; (b) drafting the article or revising it critically for important intellectual content; and (c) approval of the final version.

Compliance with Ethical Standards

Conflict of interest The authors have no affiliation with any organization with a direct or indirect financial interest in the subject matter discussed in the manuscript.

References

1. Lail BA, Hamed O, Deghles A, Qasem B, Azzaoui K, Obied AA, Algarra M, Jodeh S (2019) Environ Sci Pollut Res 26:28080
2. Haseena M, Malik MF, Javed A, Arshad S, Asif N, Zulfiqar S, Hanif J (2017) Environ Risk Assess Remediat 1:16
3. Ahmad M, Ahmed S, Swami BL, Ikram S (2015) Int J Pharmacogn 2:280
4. Gusain R, Kumar N, Fosso-Kankeu E, Ray SS (2019) ACS Omega 4:13922
5. Singha B, Das SK (2012) Environ Sci Pollut Res 19:2212
6. Barakat M (2011) Arab J Chem 4:361
7. Abdulrazak S, Hussaini K, Sani HM (2017) Appl Water Sci 7:3151
8. Wołowiec M, Komorowska-Kaufman M, Pruss A, Rzepa G, Bajda T (2019) Minerals 9:487
9. Ince M, Ince OK (2017) Int J Pure Appl Sci 3:10
10. Karnib M, Kabbani A, Holail H, Olama Z (2014) Energy Procedia 50:113
11. Maleki A (2018) Ultrason Sonochem 40:460
12. Seyedi N, Saidi K, Sheibani H (2018) Catal Lett 148:277
13. Nejad MS, Seyedi N, Sheibani H (2019) Mater Chem Phys 238:121849
14. Seyedi N, Shahabi Nejad M, Saidi K, Sheibani H (2020) Appl Organomet Chem 34:e5307
15. Zarei M, Seyedi N, Maghsoudi S, Nejad MS, Sheibani H (2020) Inorg Chem Commun 2:108327
16. Zarei M, Seyedi N, Maghsoudi S, Shahabi Nejad M, Sheibani H (2020) J Chin Chem Soc 1:1
17. Erdem E, Karapinar N, Donat R (2004) J Colloid Interface Sci 280:309

18. Salavati-Niasari M, Shakouri-Arani M, Davar F (2008) Microporous Mesoporous Mater 116(1–3):77–85
19. Mortazavi-Derazkola S, Zinatloo-Ajabshir S, Salavati-Niasari M (2015) Ceram Int 41:9593
20. Najafian A, Rabbani M, Rahimi R, Deilamkamar M, Maleki A (2015) Solid State Sci 46:7
21. Al-Jlil SA (2010) Trends Appl Sci Res 5:138
22. Hajizadeh Z, Valadi K, Taheri-Ledari R, Maleki A (2020) Chem Sel 5:2441
23. Wang L, Hu G, Lyu F, Yue T, Tang H, Han H, Yang Y, Liu R, Sun W (2019) Minerals 9:281
24. El-Kafrawy AF, El-Saeed SM, Farag RK, El-Saied HAA, Abdel-Raouf MES (2017) Egypt J Pet 26:23
25. Maleki A, Mohammad M, Emdadi Z, Asim N, Azizi M, Safaei J (2020) Arab J Chem 13:3017
26. Maleki A, Hajizadeh Z, Sharifi V, Emdadi ZA (2019) J Clean Prod 215:1233
27. Emdadi Z, Asim N, Amin MH, Ambar Yarmo M, Maleki A, Azizi M, Sopian K (2017) Appl Sci 7:514
28. Al-Harahsheh MS, Al Zboon K, Al-Makhadmeh L, Hararah M, Mahasneh M (2015) J Environ Chem Eng 3:1669
29. Sekhar KC, Kamala C, Chary N, Anjaneyulu Y (2003) Int J Miner Process 68:37
30. Esmaeili E, Salavati-Niasari M, Mohandes F, Davar F, Seyghalkar H (2011) Chem Eng J 170:278
31. Salavati-Niasari M, Davar F, Fereshteh Z (2009) Chem Eng J 146:498
32. Salavati-Niasari M, Banitaba SH (2003) J Mol Catal A Chem 201:43
33. Maleki A, Rahimi R, Maleki S (2016) Environ Chem Lett 14:195
34. Rabbani M, Bathaee H, Rahimi R, Maleki A (2016) Desalin Water Treat 57:25848
35. Ahmadian-Fard-Fini S, Ghanbari D, Salavati-Niasari M (2019) Compos Part B Eng 161:564
36. Ahmadian-Fard-Fini S, Ghanbari D, Amiri O, Salavati-Niasari M (2020) Carbohydr Polym 229:115428
37. Rostami-Vartooni A, Nasrollahzadeh M, Salavati-Niasari M, Atarod M (2016) J Alloys Compd 689:15
38. Salavati-Niasari M, Farzaneh F, Ghandi M (2020) J Mol Catal A Chem 186:101
39. Salavati-Niasari M, Hasanalian J, Najafian H (2004) J Mol Catal A Chem 209:209
40. Singha A, Guleria A (2014) Int J Biol Macromol 67:409
41. Zahedifar M, Shirani M, Akbari A, Seyedi N (2019) Cellulose 26:6797
42. Mohanty A, Drzal LT, Misra M (2002) J Polym Environ 10:19–26
43. Klemm D, Fink HP, Heublein B, Bohn A (2005) Angew Chem Int 44:3358
44. Zhong Y, Godwin P, Jin Y, Xiao H (2020) Adv Ind Eng Polym Res 3:27
45. Zhang C, Su J, Zhu H, Xiong J, Liu X, Li D, Chen Y, Li Y (2017) RSC Adv 7:34182
46. Jamshaid A, Hamid A, Muhammad N, Naseer A, Ghaur M, Iqbal J, Rafiq S, Shah NS (2017) ChemBioEng Rev 4:240
47. Gao X, Zhang H, Chen K, Zhou J, Liu Q (2018) Cellulose 25:2531
48. Strong EB, Kirschbaum CW, Martinez AW, Martinez NW (2018) Cellulose 25:3211
49. Errokh A, Magnin A, Putaux JL, Boufi S (2018) Cellulose 25:3899
50. Chen D, van de Ven TGM (2016) Cellulose 23:1051
51. Kim UJ, Ro Lee Y, Kang TH, Weon Choi J, Kimura S, Wada M (2017) Carbohydr Polym 163:34
52. Saravanan R, Ravikumar L (2017) Water Environ Res 89:629
53. Naeimi A, Honarmand M, Omid J (2018) Cell Chem Technol 52:5
54. Zhang S, Liu B, Hu D, Zhang S, Pei Y, Gong Z (2020) Anal Chim Acta 1139:189
55. Mehdaoui R, Chaabane L, Beyou E, Baouab MHV (2019) J Iran Chem Soc 16:645
56. Das K, Ray D, Bandyopadhyay NR, Sengupta S (2010) J Polym Environ 18:355
57. Kadumudi FB, Trifol J, Jahanshahi M, Zsurzsan TG, Mehrali M, Zeqiraj E, Shaki H, Alehosseini M, Gundlach C, Li Q, Dong M (2020). ACS Appl Mater Interfaces. https://doi.org/10.1021/acsami.0c15326
58. Ciolacu D, Ciolacu F, Popa VI (2011) Cellul Chem Technol 45:13
59. Naiya TK, Bhattacharya AK, Das SK (2009) J Colloid Interface Sci 333:14–26
60. Kadirvelu K, Namasivayam C (2003) Adv Environ Res 7:471
61. Ramesh A, Hasegawa H, Maki T, Ueda K (2007) Sep Purif Technol 56:90
62. Ho YS, Mckay G (1998) Chem Eng J 70:115
63. Tütem E, Apak MR, Unal ÇF (1998) Water Res 32:2315
64. Ho YS, Mckay G (1999) Process Biochem 34:451
65. Yang X, Al-Duri BA (2005) J Colloid Interface Sci 287:25
66. Rao MM, Chandra Purna GP, Seshaiah K, Nette VC, Wang M (2008) Waste Manag 28:849
67. Ho YS, Mckay G (1998) Process Saf Environ 76:332
68. Brdar M, Šćíban MB, Takaĉi AA, Došenović TM (2012) Chem Eng J 183:108
69. Freundlich H (1906) J Phys Chem 57:385–471
70. Ma Z, Kotaki M, Ramakrishna SA (2005) J Membr Sci 265:115
71. Wang Z, Mao M, Wang X, Li S, Liu Y, Yang G (2020) Carbohydr Polym 232:115781
72. Kardam A, Raj KR, Srivastava S, Srivastava MM (2014) Clean Technol Environ 16:385–393
73. Gyananath G, Balhal D (2012) Cell Chem Technol 46:121
74. Tirtom VN, Dinçer A, Becerik S, Aydemir T, Celik A (2012) Desalin Water Treat 39:76
75. Shukla SR, Pai RS (2005) J Chem Technol Biotechnol 80:176
76. O'Connell DW, Birkinshaw C, O'Dwyer TF (2006) Adsorpt Sci Technol 24:337
77. Aoki N, Fukushima K, Kurakata H, Sakamoto M, Furuhata K (1999) React Funct Polym 42:223
78. Zhao G, Zhang H, Fan Q, Ren X, Li J, Chen Y, Wang X (2010) J Hazard Mater 173:661
79. Argun ME, Dursun S, Özdemir C, Karatas M (2007) J Hazard Mater 141:77
80. Dos Reis LGT, Robaina NF, Pacheco WF, Cassella RJ (2011) Chem Eng 171:532
81. Nollet H, Roels M, Lutgen P, Van der Meeren P, Verstraete W (2003) Chemosphere 53:655
82. Zhou D, Zhang L, Guo S (2005) Water Res 39:3755
83. Chen Q, Zheng J, Wen L, Yang C, Zhang LA (2019) Chemosphere 224:509
84. Kozuch S, Martin JM (2012) ACS Catal 2:2787
85. Kozuch S (2012) Comput Mol Sci 2:795
86. Kozuch S, Shaik S (2008) J Phys Chem A 112:6032
87. Dhiman M, Chalke B, Polshettiwar V (2017) J Mater Chem 5:1935
88. Yang XF, Wang A, Qiao B, Li J, Liu J, Zhang T (2013) Acc Chem 46:1740

Terms and Conditions

Springer Nature journal content, brought to you courtesy of Springer Nature Customer Service Center GmbH (“Springer Nature”).
Springer Nature supports a reasonable amount of sharing of research papers by authors, subscribers and authorised users (“Users”), for small-scale personal, non-commercial use provided that all copyright, trade and service marks and other proprietary notices are maintained. By accessing, sharing, receiving or otherwise using the Springer Nature journal content you agree to these terms of use (“Terms”). For these purposes, Springer Nature considers academic use (by researchers and students) to be non-commercial.
These Terms are supplementary and will apply in addition to any applicable website terms and conditions, a relevant site licence or a personal subscription. These Terms will prevail over any conflict or ambiguity with regards to the relevant terms, a site licence or a personal subscription (to the extent of the conflict or ambiguity only). For Creative Commons-licensed articles, the terms of the Creative Commons license used will apply.
We collect and use personal data to provide access to the Springer Nature journal content. We may also use these personal data internally within ResearchGate and Springer Nature and as agreed share it, in an anonymised way, for purposes of tracking, analysis and reporting. We will not otherwise disclose your personal data outside the ResearchGate or the Springer Nature group of companies unless we have your permission as detailed in the Privacy Policy.
While Users may use the Springer Nature journal content for small scale, personal non-commercial use, it is important to note that Users may not:

1. use such content for the purpose of providing other users with access on a regular or large scale basis or as a means to circumvent access control;
2. use such content where to do so would be considered a criminal or statutory offence in any jurisdiction, or gives rise to civil liability, or is otherwise unlawful;
3. falsely or misleadingly imply or suggest endorsement, approval , sponsorship, or association unless explicitly agreed to by Springer Nature in writing;
4. use bots or other automated methods to access the content or redirect messages
5. override any security feature or exclusionary protocol; or
6. share the content in order to create substitute for Springer Nature products or services or a systematic database of Springer Nature journal content.

In line with the restriction against commercial use, Springer Nature does not permit the creation of a product or service that creates revenue, royalties, rent or income from our content or its inclusion as part of a paid for service or for other commercial gain. Springer Nature journal content cannot be used for inter-library loans and librarians may not upload Springer Nature journal content on a large scale into their, or any other, institutional repository.
These terms of use are reviewed regularly and may be amended at any time. Springer Nature is not obligated to publish any information or content on this website and may remove it or features or functionality at our sole discretion, at any time with or without notice. Springer Nature may revoke this licence to you at any time and remove access to any copies of the Springer Nature journal content which have been saved.
To the fullest extent permitted by law, Springer Nature makes no warranties, representations or guarantees to Users, either express or implied with respect to the Springer nature journal content and all parties disclaim and waive any implied warranties or warranties imposed by law, including merchantability or fitness for any particular purpose.
Please note that these rights do not automatically extend to content, data or other material published by Springer Nature that may be licensed from third parties.
If you would like to use or distribute our Springer Nature journal content to a wider audience or on a regular basis or in any other manner not expressly permitted by these Terms, please contact Springer Nature at

onlineservice@springernature.com